Effects of Flow Transients on the Burning Velocity of Hydrogen-Air Premixed Flames*

HONG G. IM and JACQUELINE H. CHEN
Combustion Research Facility
Sandia National Laboratories, Livermore, CA 94551

Corresponding author:
Dr. Hong G. Im
Combustion Research Facility, MS 9051
Sandia National Laboratories
Livermore, CA 94551-0969, USA

Phone: (925) 294-3131
Fax: (925) 294-2595
email: hgim@heptane.ca.sandia.gov

Word Count:
Text: 3300 (estimate 300 words/page × 11 pages)
References: 280 (40 lines × 7 words)
Tables: 100
Figures: 1800 (9 × 200)
Total: 5480

Preferred Presentation:
Oral

Preferred colloquium topic area:
Laminar Flames

*Submitted to the 28th Symposium (International) on Combustion, University of Edinburgh, Scotland, July 30 - August 4, 2000.

DISCLAIMER

DISCLAIMER

Portions of this document may be illegible in electronic image products. Images are produced from the best available original document.

Abstract

The effects of unsteady strain rate on the burning velocity of hydrogen-air premixed flames are studied in an opposed nozzle configuration. The numerical method employs adaptive time integration of a system of differential-algebraic equations. Detailed hydrogen-air kinetic mechanism and transport properties are considered. The equivalence ratio is varied from lean to rich premixtures in order to change the effective Lewis number. Steady Markstein numbers for small strain rate are computed and compared with experiment. Different definitions of flame burning velocity are examined under steady and unsteady flow conditions. It is found that, as the unsteady frequency increases, large deviations between different flame speeds are noted depending on the location of the flame speed evaluation. Unsteady flame response is investigated in terms of the Markstein transfer function which depends on the frequency of oscillation. In most cases, the flame speed variation attenuates at higher frequencies, as the unsteady frequency becomes comparable to the inverse of the characteristic flame time. Furthermore, unique resonance-like behavior is observed for a range of rich mixture conditions, consistent with previous studies with linearized theory.

Introduction

In the laminar flamelet regime of turbulent premixed combustion, the turbulent burning velocity is determined by the integral of the local laminar flamelet speed over the entire flame front which is corrugated by the turbulent eddies. It is well known that the laminar flame speed is not a constant, but a function of flame stretch, consisting of strain and curvature components induced by the turbulent flow. There are also flame instability modes that contribute to an enhanced surface area. Therefore, it is important to understand and parameterize the effect of stretch on the flame speed in accurately predicting the overall burning rate of premixed combustion devices.

Through a number of theoretical and experimental studies over the past decades, it has been fairly well established that the flame speed, S, is linearly proportional to stretch in the weak stretch limit. This relation is written in nondimensional form as:

$$S/S_L = 1 - MaKa \tag{1}$$

where S_L is the unstretched laminar flame speed, Ka is the Karlovitz number representing stretch, and Ma is the proportionality constant known as the Markstein number [1]. Asymptotic analysis showed that the Markstein number is a function of thermodynamic and transport properties of the mixture [2, 3, 4], such that it can assume positive or negative values depending on the diffusivity of the deficient reactant species, known as the Lewis number effect. Experimental measurements have been performed to confirm this prediction [5, 6, 7, 8], while computational studies with detailed chemical kinetics and transport provided means to extract accurate values of the Markstein numbers for various fuel mixtures [9, 10].

Most of the previous studies regarding the stretch effect on premixed flames, however, are based on quasi-steady flames and hence may become inaccurate in highly transient

flows produced by turbulence. The effect of unsteady flow on premixed flame propagation was investigated in asymptotic studies [11, 12] where it was found that the flame speed becomes independent of strain in the high frequency limit, while the curvature component remains. Recent direct numerical simulation of turbulent methane-air [13] and hydrogen-air [14] premixed flames also revealed that the flame speed response becomes less sensitive to turbulent flows for higher turbulence intensities. These results clearly suggest that flow unsteadiness is an important parameter in controlling the premixed flame response.

In this paper, we present a parametric study on the response of premixed flames with detailed hydrogen-air chemistry to unsteady strain rate. Effects of thermo-diffusive imbalance are investigated by comparing the results for different equivalence ratios. Various definitions of the flame speed arising from finite flame structure are also discussed. The results are compared with theoretical predictions and some recent experimental measurements.

Formulation and Numerical Method

The numerical configuration is a counterflow system between two opposing axisymmetric nozzles separated by a distance of L. Following the previous work [15, 16], a modified system of equations for the unsteady problem is adopted in order to take into account the high-index nature of the problem, thereby facilitating numerical integration using adaptive time integration. Defining the self-similar variables for the axial velocity, scaled radial velocity, temperature and species mass fractions as:

$$u = u(t, x), \quad v/r = V(t, x), \quad T = T(t, x), \quad Y_k = Y_k(t, x), \tag{2}$$

and introducing the acoustic pressure, $p = P - p_0$, where P is the total static pressure and p_0 is the thermodynamic pressure, the conservation equations are written as:

Mass continuity:

$$\frac{\rho}{P}\frac{\partial p}{\partial t} - \frac{\rho}{T}\frac{\partial T}{\partial t} - \rho\overline{W}\sum_k \frac{1}{W_k}\frac{\partial Y_k}{\partial t} + \frac{\partial}{\partial x}(\rho u) + 2\rho V = 0, \tag{3}$$

Axial momentum:

$$\rho\frac{\partial u}{\partial t} + \rho u\frac{\partial u}{\partial x} + \frac{\partial p}{\partial x} - 2\mu\frac{\partial V}{\partial x} - \frac{4}{3}\frac{\partial}{\partial x}\left(\mu\frac{\partial u}{\partial x}\right) + \frac{4}{3}\frac{\partial}{\partial x}(\mu V) = 0, \tag{4}$$

Radial momentum:

$$\rho\frac{\partial V}{\partial t} + \rho u\frac{\partial V}{\partial x} + \rho V^2 - \frac{\partial}{\partial x}\left(\mu\frac{\partial V}{\partial x}\right) + \Lambda = 0, \tag{5}$$

Energy conservation:

$$\rho c_p\frac{\partial T}{\partial t} + \rho c_p u\frac{\partial T}{\partial x} - \frac{\partial}{\partial x}\left(\lambda\frac{\partial T}{\partial x}\right) - \frac{\partial P}{\partial t} + \rho(\sum_k c_p Y_k V_k)\frac{\partial T}{\partial x} + \sum_k h_k W_k\omega_k = 0, \tag{6}$$

Species conservation:

$$\rho\frac{\partial Y_k}{\partial t} + \rho u\frac{\partial Y_k}{\partial x} + \frac{\partial}{\partial x}(\rho Y_k V_k) - W_k\omega_k = 0, \quad k = 1, \cdots, K. \tag{7}$$

The equation of state becomes

$$\rho = (p + p_0)\,\overline{W}/RT. \tag{8}$$

In the above equations, c_p is the specific heat of the mixture, λ is the thermal conductivity of the mixture, h_k is the enthalpy of species k, W_k is the molecular weight of species k, and ω_k is the molar reaction rate for species k. The above system of differential-algebraic equations is integrated using DASPK [17], which employs a backward-difference formula method with adaptive time-step and order control. The code interacts with Chemkin [18] and Transport [19] packages for computing reaction rates and transport properties. The kinetic mechanism used is the hydrogen-air system developed by Yetter *et al.* [20].

For the boundary conditions, fresh reactants at 300 K are supplied at $x = L$ and burnt product is supplied at $x = 0$, where the temperature and composition of the product is determined from the downstream values of the freely-propagating premixed flame for the given fresh mixture condition at $x = L$. The scaled radial velocity, V, is set to zero at both boundaries, and the unsteady flow field is imposed by specifying the equal axial velocity at both boundaries as a function of time. A sinusoidal velocity of the form

$$u(x = 0) = -u(x = L) = u_0\{1 + A[1 - \cos(2\pi f t)]\} \tag{9}$$

is imposed such that the velocity oscillates from u_0 to $u_0(1 + 2A)$ at a frequency of f Hz, which is a parameter characterizing the unsteady flow time scale.

Various Definitions of the Flame Speed

While the mathematical definition for the flame speed and strain rate is based on an asymptotically thin reaction zone, in reality the flame has a finite thickness such that these quantities cannot be uniquely defined. In many counterflow experiments [21], the flame speed has been measured at the leading edge of the preheat zone, which is identified as the local maximum of the axial velocity profile. This upstream velocity, denoted as S_u herein, is relatively easy to measure using laser doppler velocimetry. A recent experimental study of unsteady premixed flames [22] also followed this convention. As will be discussed later, however, under unsteady conditions such a definition can lead to significantly different results compared to other definitions as the unsteady frequency increases.

In numerical studies with finite rate chemistry, more mathematically rigorous definitions have been suggested [23]. The displacement speed, derived from the Hamilton-Jacobi equation, is defined as the velocity of the flame surface represented by an isolevel surface of a

chosen species. To minimize thermal expansion effects across the flame, the density-weighted displacement speed, S_d, for species k is defined as [24]

$$S_d \equiv -\frac{W_k \omega_k}{\rho_u \, |\nabla Y_k|} - \frac{\frac{\partial}{\partial \eta}\left(\rho D_k \frac{\partial Y_k}{\partial \eta}\right)}{\rho_u \, |\nabla Y_k|} - \frac{\rho D_k}{\rho_u}(\nabla \cdot \mathbf{n}), \tag{10}$$

where ρ_u is the density of the upstream reactant mixture, D_k is the mass diffusivity of species k, and η is the coordinate normal to the flame front. The last term in Eq. (10) represents the effect of flame curvature, $\nabla \cdot \mathbf{n}$, where $\mathbf{n} = -\nabla Y_k / |\nabla Y_k|$ is the unit vector normal to the front. One disadvantage of this definition is that the displacement speed depends on the choice of the isolevel surface, although it was observed that the variation is relatively small when the isolevel surface is near the reaction zone [13].

The consumption speed is also defined [23] as a measure of the consumption rate of species k per unit flame area, written as

$$S_c \equiv \frac{\int \dot{\omega}_k d\eta}{\rho_u (Y_{k,b} - Y_{k,u})}, \tag{11}$$

where subscripts u and b denote the unburnt and burnt sides, respectively. This quantity is directly related to the overall burning rate and can be of practical importance.

The primary focus of this paper is the effect of strain rate on the flame speed. For the axisymmetric counterflow, the Karlovitz number represents the strain component only, and is defined as

$$Ka = \frac{\delta \kappa}{S_L} \tag{12}$$

where

$$\kappa = \frac{1}{r}\frac{\partial}{\partial r}(v) \tag{13}$$

and δ is the flame thickness. Note that the Karlovitz number varies significantly in magnitude depending on the definition of the flame thickness. We choose $\delta = D_k / S_L$ where D_k is

the mass diffusivity of species k with respect to the upstream conditions for mixture and temperature. For the results presented herein, O_2 is chosen for the marker species.

Steady Response

As a reference point, we compute the steady response of premixed flames of hydrogen-air mixture with various equivalence ratios. For each mixture condition, we compare various definitions of the flame speed described in the previous section. As an example, Fig. 1 shows the result for a lean mixture of $\phi = 0.4$. The solid lines denote the displacement speed evaluated at four different values of the O_2 mass fraction, where the maximum heat release occurs approximately at $Y_{O_2} = 0.17$. Although qualitatively similar, the four values lead to quantitatively different results for S_d. The consumption speed, which is uniquely defined for a given species, falls within the S_d curves with the same qualitative trend, while S_u, the flame speed based on the location far upstream, tends to significantly overestimate the result. The strain rate given by Eq. (13) is computed at the chosen Y_{O_2} isocontour for S_d. Since no specific isocontour is needed to compute S_c and S_u, the strain rate value at $Y_{O_2} = 0.17$ is used here.

Results for the Markstein number obtained from a linear curve fit for various flame speed definitions are plotted in Fig. 2. The range of Ka is limited to smaller values, approximately $Ka < 0.2$ for the definition based on D_{O_2}. The experimental results by Aung *et al.*[7] are also converted and plotted. Quantitative discrepancies may be attributed to the different geometry and chemical/transport data. Nevertheless, the Markstein numbers based on S_d and S_c capture the general qualitative trend in terms of 1) the leveling-off behavior on the rich side, and 2) the crossover point in the equivalence ratio where the Markstein number changes sign, which occurs in the lean mixture near $\phi = 0.6 \sim 0.7$. On the other hand, the Markstein

number based on S_u is always negative and appears to be inadequate in capturing the strain effect on the flame speed. This issue has also been discussed in a previous study [25]. Further discrepancies in S_u caused by flow unsteadiness will be discussed in the next section.

Response to Oscillatory Strain Rate

We perform a series of calculations for premixed flames with different mixture conditions subjected to an oscillatory velocity field given by Eq. (9). Table 1 shows the parametric values for the various test cases. Each case is computed for various frequencies, mostly ranging from 1 to 1000 Hz. In response to the velocity oscillation, both strain rate and flame speed fluctuate in time. After a number of cycles, the solution approaches a limit cycle in a phase space of flame speed versus strain rate.

Figure 3(a) shows the result for the $\phi = 0.4$ case, representing a typical flame speed response. As the frequency of oscillation increases, responses of both S_c and Ka are attenuated, resulting in a reduced size of the limit cycle in Fig. 3(a). Moreover, the increased phase delay of the flame response to strain rate causes tilting of the response curve, resulting in a smaller Markstein number (the slope of the ellipse). The result of the flame response attenuation is consistent with previous studies of unsteady flames [26, 27]. Although not shown here, the response of S_d to unsteady strain is similar to either that of S_c.

The response of S_u plotted in Fig. 3(b), however, shows drastically different results from that of S_c or S_d. It appears as though the flame speed oscillation is amplified with increasing frequency. Such a substantial difference can be examined by comparing the velocity fields for the low and high frequency cases. Figure 4 shows a comparison of the axial velocity profiles for a quasi-steady ($f = 1$ Hz) and a high-frequency response ($f = 500$ Hz). At $f = 1$ Hz, the flame responds to the velocity fluctuation in a quasi-steady manner, such that at

any given time the solution field approaches the steady solution for the instantaneous nozzle exit velocity. As a result, there is a larger lateral displacement of the flame location and a smaller difference in the local peak velocity as u_F varies from 100 to 200 cm/s. For the high-frequency case, however, the reaction zone does not readily respond to the unsteady convective flow, leading to a smaller change in flame location and a larger fluctuation in S_u.

The aforementioned observation implies that, at high frequencies, the transient effect is balanced only by the outer convective transport, while the inner reactive zone with a shorter characteristic time scale remains largely unaffected by the unsteady oscillation. In other words, there is a segregation in the balance of the terms throughout the flame, and thus the far-upstream velocity cannot properly represent the reaction zone behavior. Incidentally, this explanation may account for the experimental observation by Hirasawa *et al.* [22], where the stretch and the flame speed fluctuation increase with frequency. In the following, the results are presented in terms of S_c, in favor of its uniqueness in definition and its physical relevance to the overall burning rate.

As derived from linearized theory [11, 12], the unsteady flame speed response to strain rate can be represented by the Markstein transfer function, defined as

$$\mathcal{M}_c = \left| \frac{S_{c,\max} - S_{c,\min}}{Ka_{\max} - Ka_{\min}} \right|, \tag{14}$$

where the subscript "min" and "max" denote the minimum and maximum values through the oscillation. It is expected that $\mathcal{M}_c$ is a function of frequency and Lewis number, which depends on the mixture composition and the amount of dilution. The frequency is normalized by the inverse of the characteristic flame time. For flames with detailed chemistry with a number of species, the proper definition of the characteristic flame time is not clear. One reasonable choice is the strain rate for the initial steady flame for each case, κ_0, as it properly

represents the characteristic flow time for the reference steady condition. The reference strain rate values are shown in Table 1.

Figures 5 shows the normalized Markstein transfer function versus the normalized frequency, $2\pi f/\kappa_0$. The transfer function for each case is normalized by its quasi-steady value. As the frequency increases, most of the curves fall off at the normalized frequency of order unity. This result implies that the flame speed response, for the most part, becomes less sensitive to a flow with a higher transient, consistent with the results from simplified theory [11, 12] and direct numerical simulation [13, 14].

A unique response is noted, however, for a range of fuel-rich conditions, where the transfer function exhibits a peak at a moderate frequency range before it eventually decays to zero. Such is the case for $\phi = 3.0$, and to a lesser extent, for $\phi = 5.0$, as shown in Fig. 5. To illustrate the cause for this distinct behavior, Figs. 6 (a) and (b) show a comparison of the phase-space response for $\phi = 3.0$ and 6.5. For $\phi = 6.5$, similar to the $\phi = 0.4$ case shown in Fig. 3, the ellipse tilts toward a direction such that the flame response attenuates as the frequency increases. On the other hand, for $\phi = 3.0$ case, the ellipses appear to be "tilting up" toward the vertical direction for frequencies up to $f = 2000$ Hz. For even higher frequencies, the slope starts to decrease, *e.g.* at $f = 4000$ Hz. This suggests a resonance behavior and is similar to the nonmonotonic burning rate response observed in a previous linear analysis, as discussed in Im *et al.* [27]. Similar behavior was also observed in a recent study with linearized theory [12] where the peak in the transfer function was observed for flames where the deficient species has a larger Lewis number. The present results are distinct in that such a peak response disappears again as the equivalence ratio further increases, *i.e.* for even larger Lewis numbers. On the other hand, it should be noted that an increase in the equivalence

ratio not only increases the effective Lewis number of the mixture, but also modifies the flame temperature and the heat release parameter, $\gamma = (\rho_u - \rho_b)/\rho_u$, which is another important parameter of the problem in governing the Markstein transfer function [12]. Considering that the resonance behavior is absent in the earlier study with a constant-density assumption [11], such an additional effect may be responsible for the nonmonotonic trend with respect to the equivalence ratio.

To further assess the dilution effect, Fig. 7 shows a comparison of the Markstein transfer function for undiluted and diluted cases for $\phi = 3.0$. The undiluted case is the result from Fig. 5 while the diluted case corresponds to air diluted with nitrogen, $O_2/(O_2 + N_2) = 0.114$ by volume, such that the flame speed and temperature are substantially reduced (see Table 1). The resonance behavior observed for the undiluted case is substantially suppressed with dilution, although some nonmonotonic response remains at similar values of the normalized frequency. The results suggests that both mixture Lewis number and heat release parameter contribute to the nonmonotonic flame response to unsteady strain rate.

Conclusions

The response of hydrogen-air premixed flames to oscillatory strain rates have been studied in an opposed nozzle configuration. It was found that, while expedient for experimental measurements, the upstream local peak value of the axial velocity, S_u, is inadequate in representing the burning velocity characteristics for highly transient flames due to the inability of the reaction layer to respond to the rapid transients in the convective transport zone. The displacement speed, S_d, is useful in describing the flame as a front, but the results depend on the specific choice of the isolevel surface. The consumption speed, S_c, does not suffer from the ambiguity of location, and is thus mainly examined as a measure of the integrated

burning velocity.

The Markstein transfer function versus the frequency of oscillation has also been investigated for mixtures with various equivalence ratios. The general trend is that the flame speed response to strain rate fluctuation attenuates as the frequency exceeds the inverse of the characteristic flame time, consistent with many previous studies on unsteady diffusion/premixed flames. Unique behavior was observed, however, for some rich mixtures, in which the transfer function exhibits a peak response for moderate frequencies. This distinct behavior disappears again as the equivalence ratio is further increased, possibly due to the effect of the reduced heat-release parameter. Further comparison of the Markstein transfer function to the case with dilution revealed that the resonance response is suppressed by dilution.

Acknowledgment

This work was supported by the United States Department of Energy, Office of Basic Energy Sciences, Chemical Sciences Division. The authors thank Professors L. L. Raja and R. J. Kee of Colorado School of Mines and Dr. A. E. Lutz of Sandia National Laboratories for their assistance in developing the computational method.

References

[1] Markstein, G. H., *Non-steady Flame Propagation*, MacMillan, New York, 1964.

[2] Clavin, P. and Williams, F. A., *J. Fluid Mech.*, 116:251-282 (1982).

[3] Pelce, P. and Clavin, P., *J. Fluid Mech.*, 124:219-237 (1982).

[4] Matalon, M. and Matkowsky, B. J., *J. Fluid Mech.*, 124:239-259 (1982).

[5] Searby, G. and Quinard, J., *Combust. Flame*, 82:298-311 (1990).

[6] Tseng, L.-K., Ismail, M. A. and Faeth, G. M., *Combust. Flame*, 95:410-426 (1993).

[7] Aung, K. T., Hassan, M. I., and Faeth, G. M., *Combust. Flame*, 112:1-15 (1998).

[8] Taylor, S. C., Ph.D. thesis, University of Leeds, 1991.

[9] Müller, U. C., Bollig, M. and Peters, N., *Combust. Flame*, 108:349-356 (1997).

[10] Sun, C. J., Sung, C. J., He, L. T. and Law, C. K., *Combust. Flame*, 118:108-128 (1999).

[11] Joulin, G., *Combust. Sci. Tech.*, 97:219-229 (1997).

[12] Clavin, P. and Joulin, G., *Combust. Theory Modelling*, 1:429-446 (1997).

[13] Chen, J. H. and Im, H. G., *Twenth-Seventh Symposium (International) on Combustion*, The Combustion Institute, Pittsburg, PA, 1998, pp. 819-826.

[14] Chen, J. H. and Im, H. G., "Stretch Effects on Various Flame Speeds in Turbulent Premixed Hydrogen-Air System," Joint Meeting of the United States Sections, The Combustion Institute, The George Washington University, Washington, DC, March 15-17, 1999.

[15] Raja, L. L., Kee, R. J., and Petzold, L. R., *Twenth-Seventh Symposium (International) on Combustion*, The Combustion Institute, Pittsburg, PA, 1998, pp. 2249-2257.

[16] Im, H. G., Raja, L. L., Kee, R. J., and Petzold, L. R., "A Numerical Study of Transient Ignition in Counterflow Nonpremixed Methane-Air System using Adaptive Time Integration," *Combust. Sci. Tech.*, submitted (1999).

[17] Li, S. and Petzold, L. R. (1999). Design of New DASPK for Sensitivity Analysis. *Technical Report of Computer Science Department* (TRCS99-23), University of California, Santa Barbara.

[18] Kee, R. J., Rupley, F. M. and Miller, J. A. (1991). Chemkin-II: A Fortran Chemical Kinetics Package for the Analysis of Gas-Phase Chemical Kinetics. *Sandia Report* SAND89-8009B.

[19] Kee, R. J., Dixon-Lewis, G., Warnatz, J., Coltrin, M. E. and Miller, J. A. (1986). A Fortran Computer Code Package for the Evaluation of Gas-Phase Multicomponent Transport Properties, *Sandia Report* SAND86-8246, December 1986.

[20] Yetter, R. A., Dryer, F. L. and Rabitz, H. (1991). A Comprehensive Reaction Mechanism for Carbon Monoxide/Hydrogen/Oxygen Kinetics, *Combust. Sci. Tech.*, 79:97-128.

[21] Egolfopoulos, F. N., Zhu, D. L., and Law, C. K., *Twenth-Third Symposium (International) on Combustion*, The Combustion Institute, Pittsburg, PA, 1990, pp. 471-478.

[22] Hirasawa, T., Ueda, T., Matsuo, A., and Mizomoto, M., *Twenth-Seventh Symposium (International) on Combustion*, The Combustion Institute, Pittsburg, PA, 1998, pp. 875-882.

[23] Poinsot, T., Echekki, T., and Mungal, G., *Combust. Sci. Tech.*, 81:45-73 (1992).

[24] Echekki, T. and Chen, J. H., *Combust. Flame*, 106:184-202 (1996).

[25] Tien, J. H. and Matalon, M., *Combust. Flame*, 84:238-248 (1991).

[26] Egolfopoulos, F. N., *Twenth-Fifth Symposium (International) on Combustion*, The Combustion Institute, Pittsburg, PA, 1994, pp. 1365-1373.

[27] Im, H. G., Bechtold, J. K., and Law, C. K., *Combust. Flame*, 105:358-372 (1996).

ϕ	S_L	D_{O_2}	u_0	A	S_c/S_L at u_0	κ_0
0.4	22.15	0.2263	100	0.5	1.553	346
0.5	59.89	0.2317	140	0.25	1.105	1220
0.7	148.50	0.2421	500	0.3	1.006	1567
3.0	258.93	0.3355	600	0.3	0.957	1781
5.0	130.38	0.3915	240	0.25	0.872	256
6.5	66.40	0.4243	120	0.5	0.315	505
3.0 (diluted)	33.25	0.2707	80	0.5	0.255	344

Table 1. Parameters for various test cases. Units for S_L and D_{O_2} are cm/s and cm^2/s, respectively. In all cases the air is undiluted, $O_2/(O_2 + N_2) = 0.21$, except for the last case denoted "diluted" where $O_2/(O_2 + N_2) = 0.114$.

List of Figures

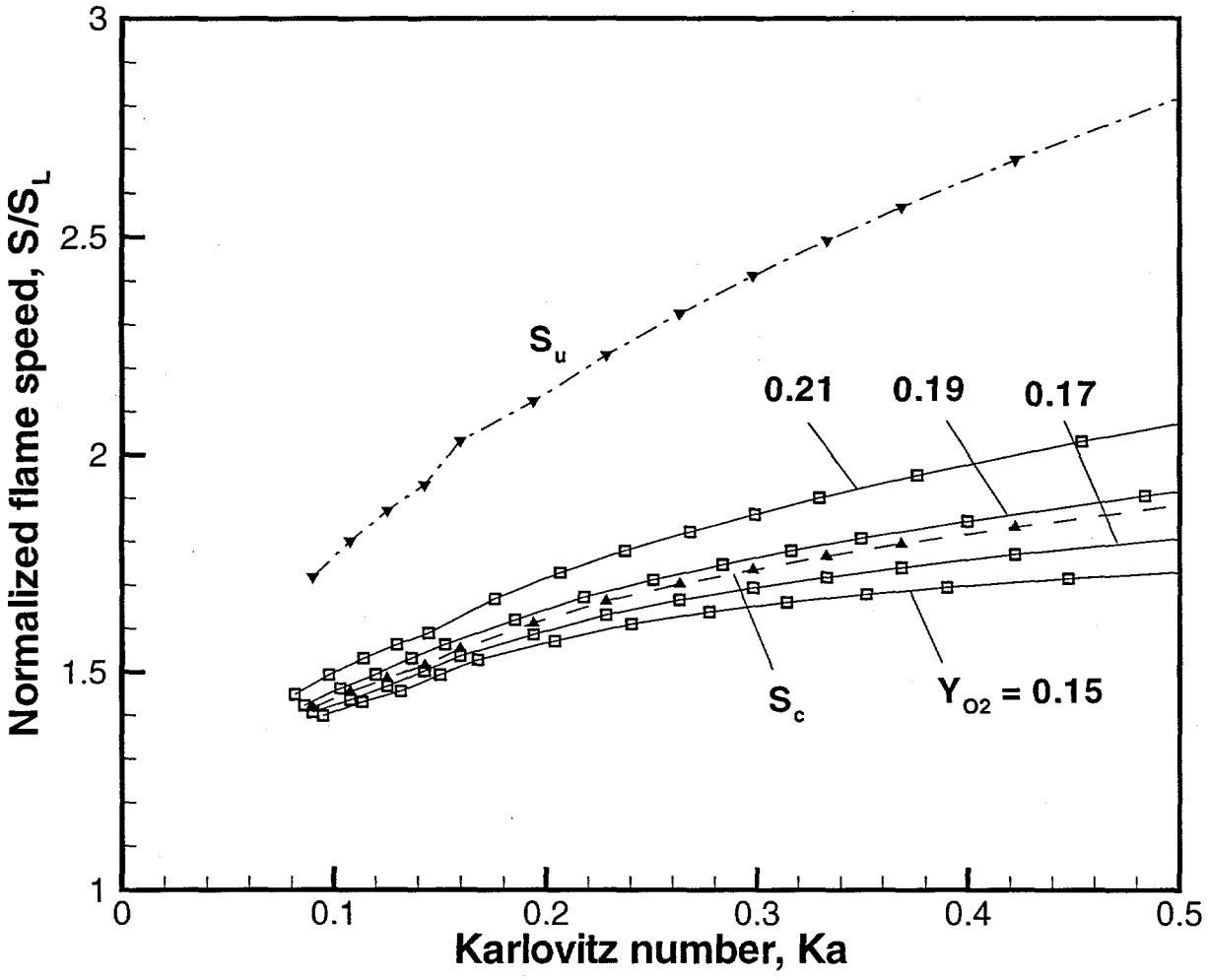

Figure 1: Steady response of various flame speeds to normalized strain rate, Ka, for $\phi = 0.4$.

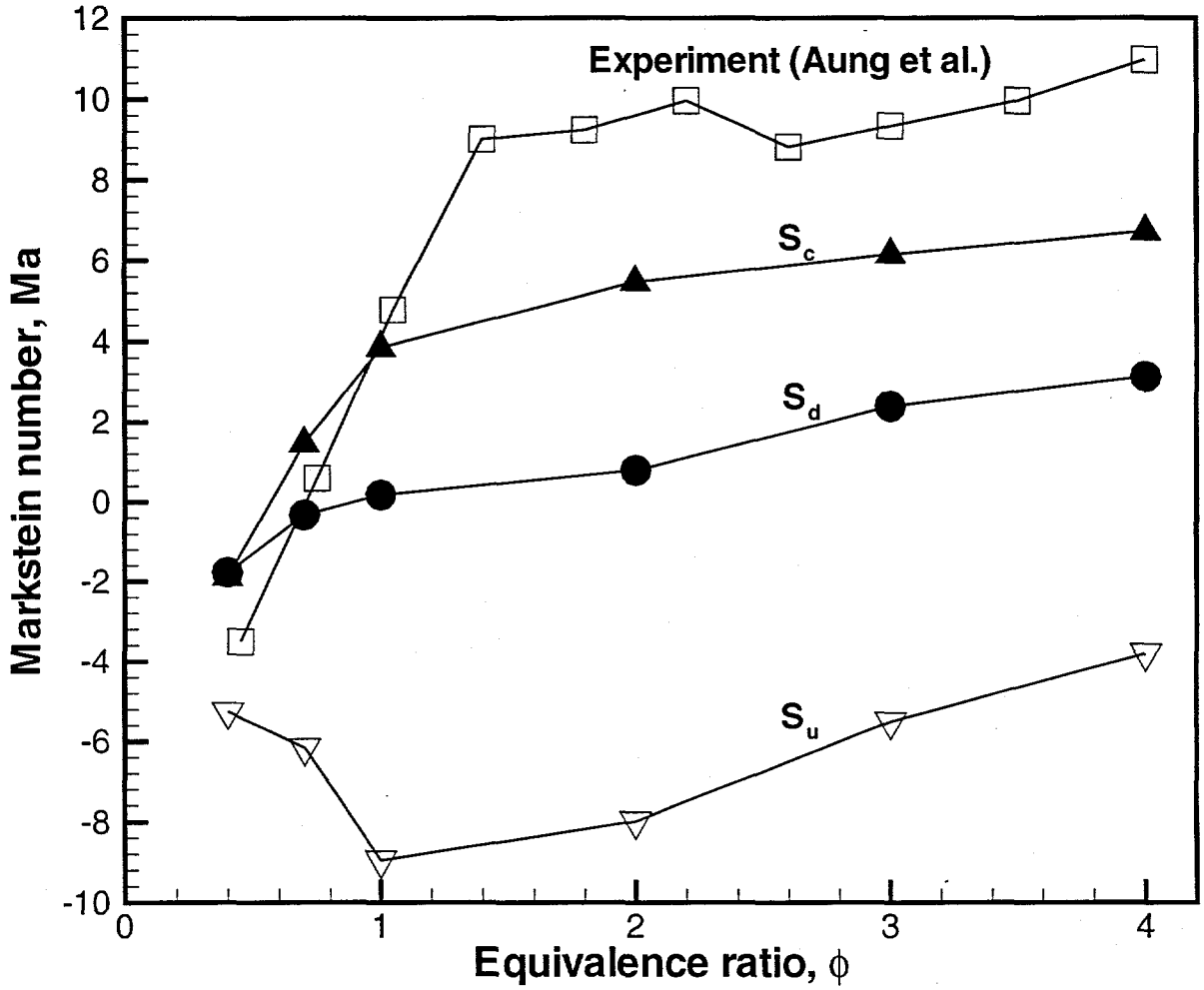

Figure 2: Markstein number based on various flame speed definitions as a function of equivalence ratio, ϕ.

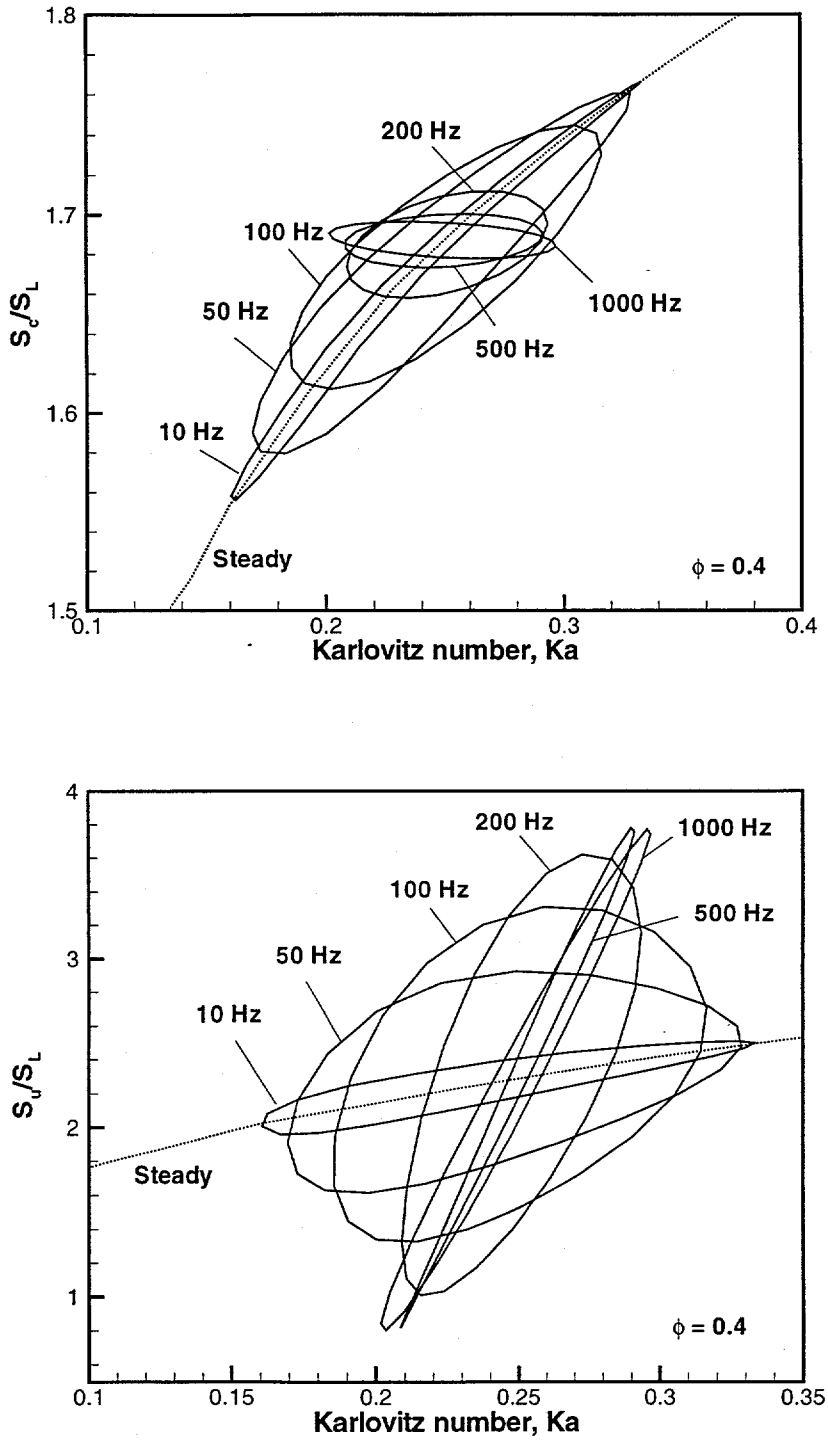

Figure 3: Response of (a) S_c and (b) S_u to the Karlovitz number, Ka, for various frequencies of oscillation; $\phi = 0.4$.

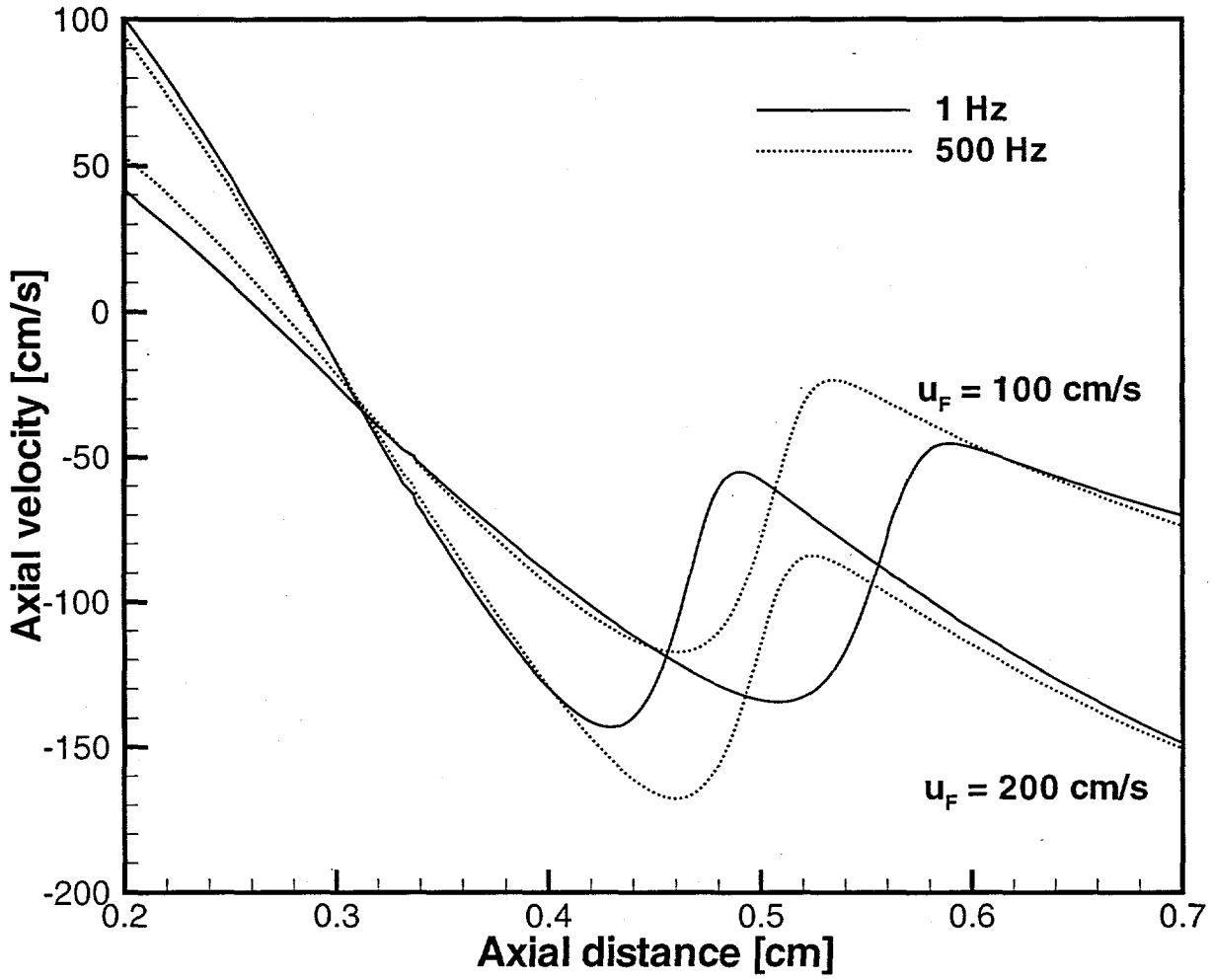

Figure 4: Comparison of the axial velocity profiles for the quasi-steady response at $f = 1$ Hz (solid lines) and for the high frequency response at $f = 500$ Hz (dotted lines), for $\phi = 0.4$. In each case, two instantaneous velocity fields at $u_F = 100$ and 200 cm/s are plotted.

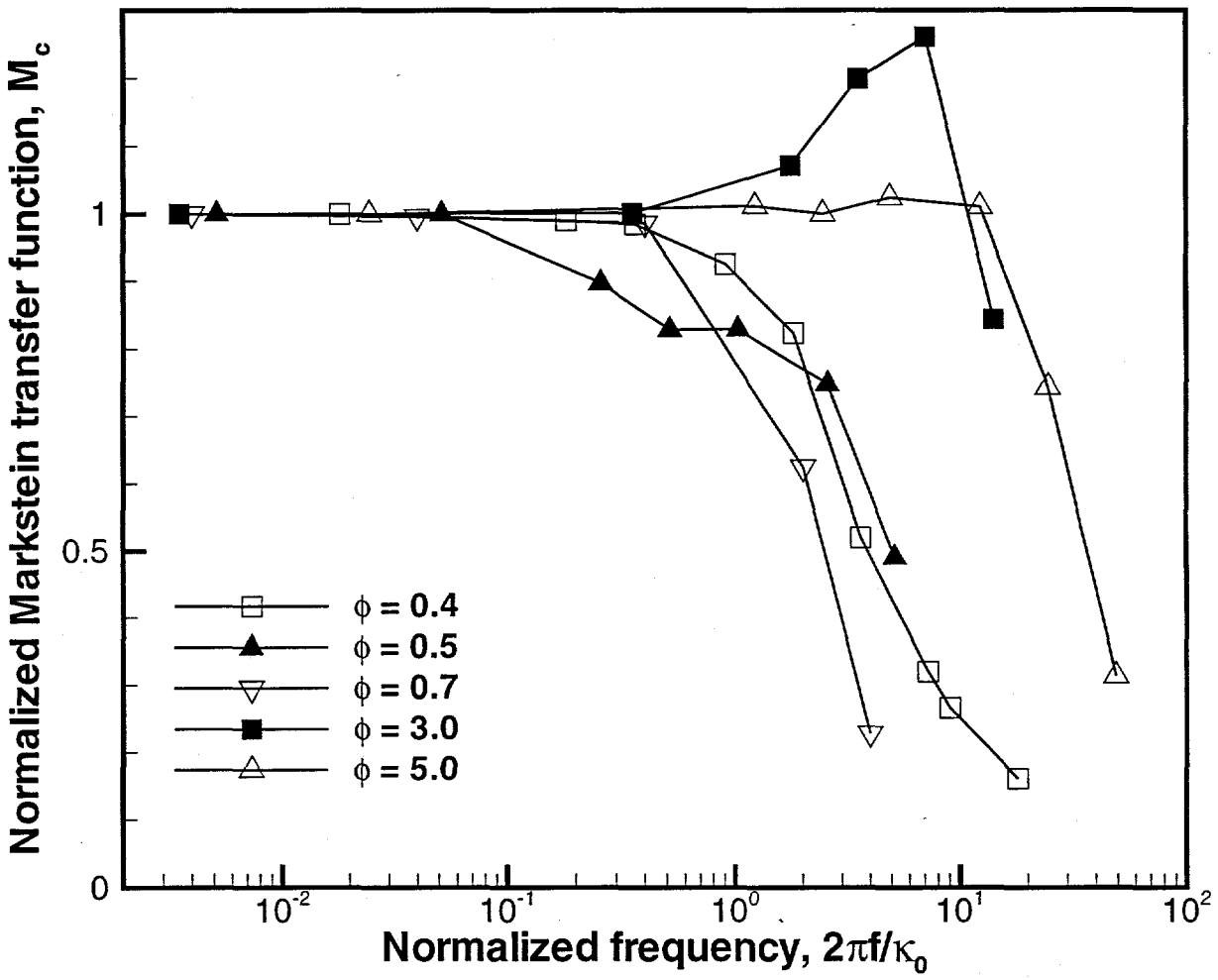

Figure 5: Normalized Markstein transfer function, $\mathcal{M}_c$, based on S_c as a function of normalized frequency, $2\pi f/\kappa_0$.

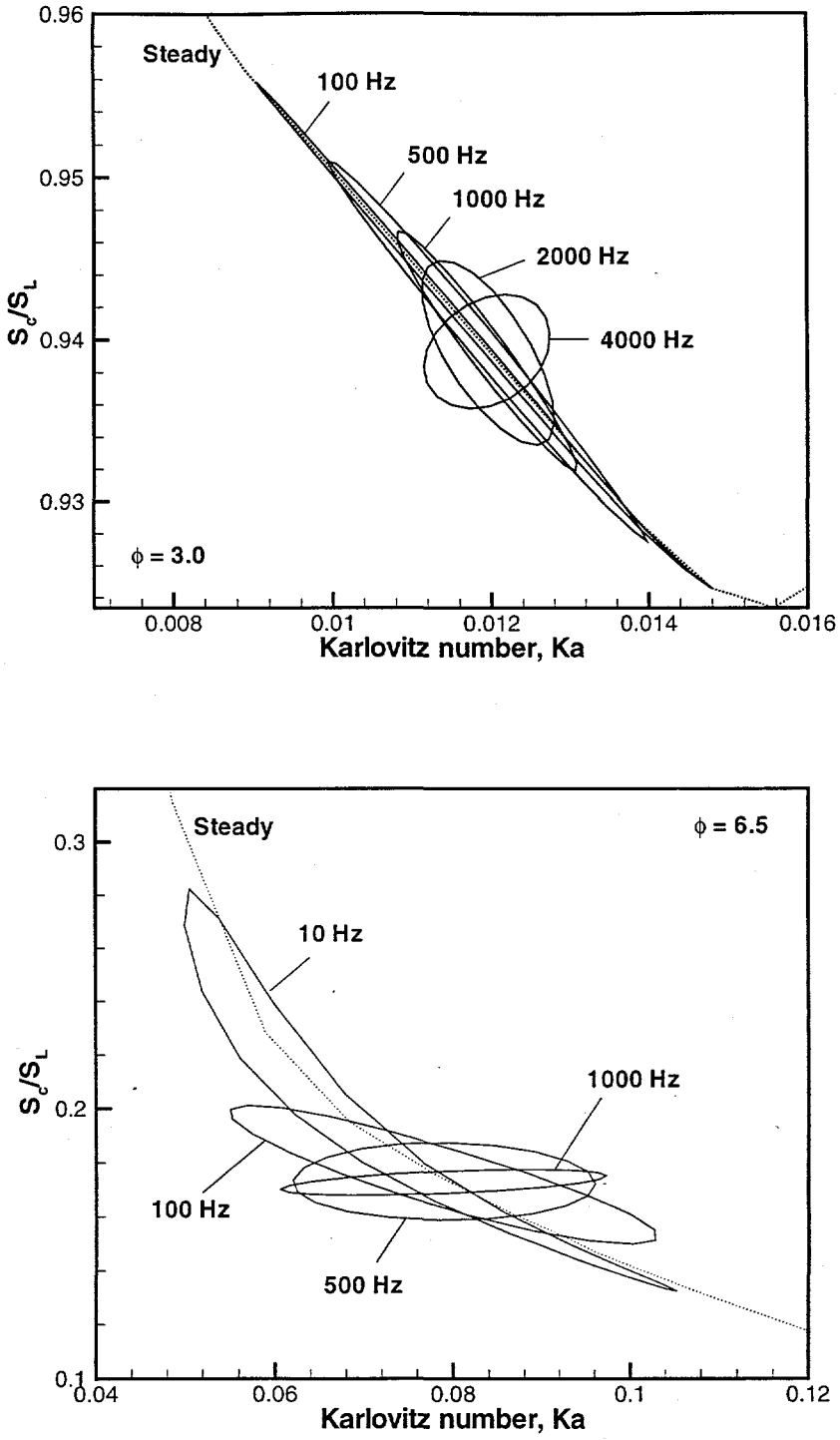

Figure 6: Response of S_c to the Karlovitz number, Ka, for various frequencies of oscillation; (a) $\phi = 3.0$, (b) $\phi = 6.5$.

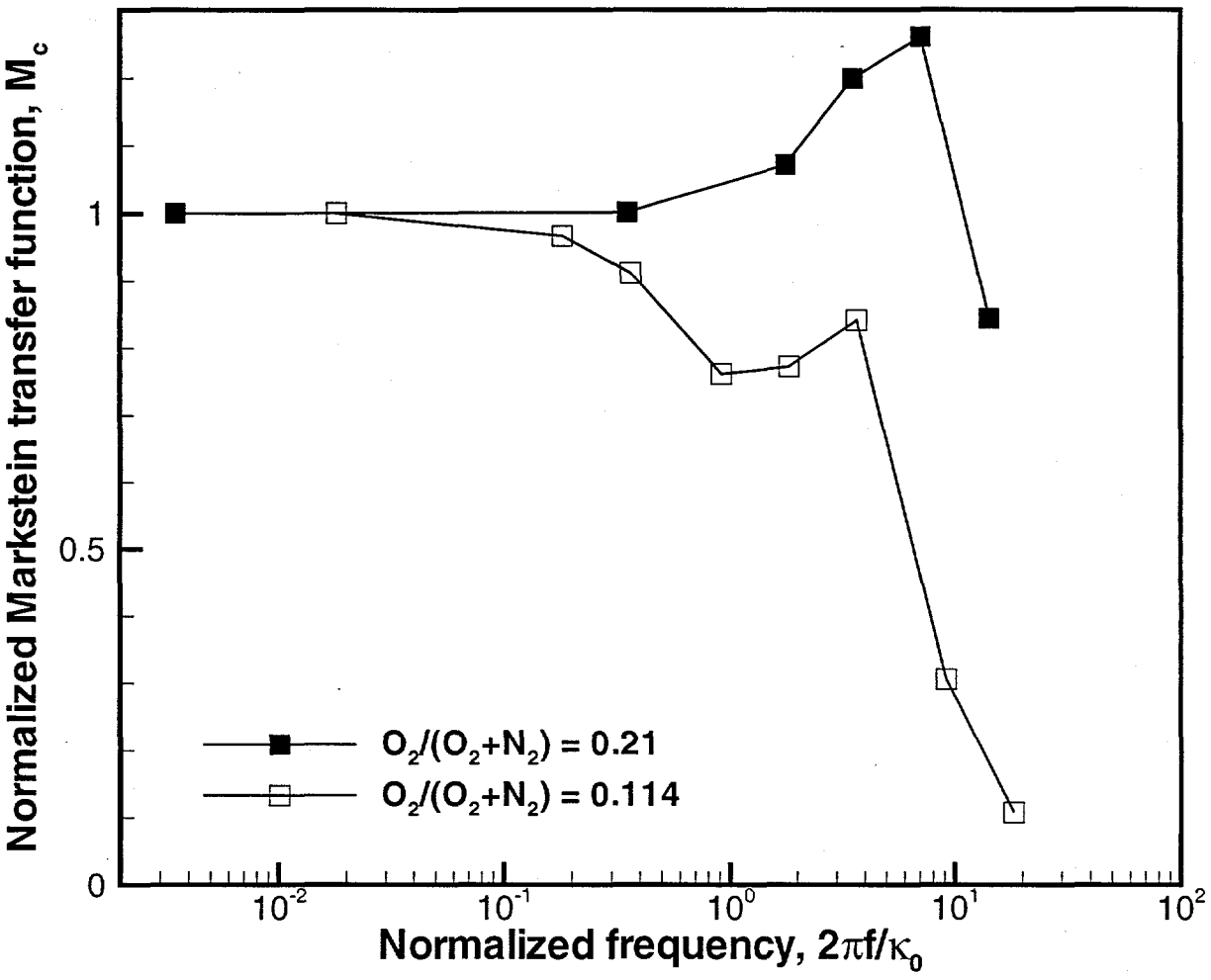

Figure 7: Normalized Markstein transfer function, $\mathcal{M}_c$, based on S_c as a function of normalized frequency, $2\pi f/\kappa_0$, for $\phi = 3.0$. Solid symbol denotes the undiluted case, $O_2/(O_2 + N_2) = 0.21$, and open symbol denotes the diluted case, $O_2/(O_2 + N_2) = 0.114$.